Synthesis and characterization of CdCr-NO$_3$ layered double hydroxides nanostructures for Cr(VI) ions adsorption: factorial design and statistical analysis for multivariate sorption optimization

Fateh Ali[a], Aydan Elçi[b], Ali Nawaz Siyal[a,*], Babar Ali Baig[a], Abdul Nabi Jakhrani[a], Sanaullah Dehraj[c], Ghansham Das[a]

[a]_Institute of Chemistry, University of Sindh, Jamshoro 76080, Pakistan, Tel. +92-22921311, Ext. 2004; email: alinsiyal@usindh.edu.pk/ alinawazsiyal@yahoo.com (A.N. Siyal), Tel. +92-22921311, Ext. 2004; email: fatehbaloch934@gmail.com (F. Ali), Tel. +92-3333832670; email: babarullah2@gmail.com (B.A. Baig), Tel. +92-22921311, Ext. 2004; email: abdulnabi4753@gmail.com (A.N. Jakhrani), Tel. +92-22921311, Ext. 2004; email: ghanshamdas2010@yahoo.com (G. Das)_
[b]_Department of Chemistry, University of Ege, Bornova 35040, Turkey, Tel: +90-2323399091; email: aydan.elci@ege.edu.tr (A. Elçi)_
[c]_Department of Mathematics and Statistics, Quaid-E-Awam University of Engineering, Science and Technology, Nawab Shah 67480, Pakistan, Tel. +923313646365; email: sanaullahdehraj@quest.edu.pk (S. Dehraj)_

ABSTRACT

In present study, nitrate anion containing CdCr layered double hydroxides (LDH) was synthesized, and characterized by Fourier transform infrared spectroscopy (FT-IR), X-ray diffraction (XRD), thermogravimetric analysis-differential scanning calorimetry (TGA-DSC) and energy-dispersive X-ray-scanning electron microscopy techniques (EDX-SEM). The characteristic diffraction peaks in the XRD pattern of CdCr-NO$_3$ LDH at 2θ values of 15.10 and 26.02° correspond to (003) and (006) planes (hkl), respectively of crystal system of the LDH, revealing layered structure of material with basal (d) spacing of d_{003}: 0.59 nm and d_{006}: 0.34 nm, containing intercalated water and nitrate anions. Stretching vibrations in FT-IR spectrum of the LDH at 3,378.01 and 1,355.51 cm^{-1} confirmed the intercalation of water and nitrate ions, respectively, in between hydrotalcite-like layers. EDX study confirmed that CdCr-NO$_3$ LDH contained 20.07%, 72.75% and 7.18% of O, Cd(II) and Cr(III), respectively. SEM image revealed that nanostructured material is porous and layered in nature. TGA-DSC confirmed the thermal stability of material at below 509.44°C. CdCr-NO$_3$ LDH was investigated as an efficient adsorbent for capturing of Cr(VI) ions form industrial effluents. The adsorption was optimized by factorial design approach. Maximum response of CdCr-NO$_3$ LDH for capturing/adsorption of Cr(VI) ions was achieved at optimum concentration of Cr(VI) ions: 10 mg L^{-1}, pH: 4.0, adsorbent amount: 40 mg and shaking time: 30 min at 25°C. Method worked well on real wastewater samples.

Keywords: Layered double hydroxides; Adsorption; Cr(VI) ions; Isotherms; Factorial design

1. Introduction

Globally, heavy metal ions contamination is emerging issue because of their genotoxicity, mutagenicity, carcinogenicity, and bioaccumulation characteristics, causing serious health and environmental problems [1]. Various heavy metals such as Cr, Ni, Zn, Cu, As, Pb, and Hg and their compounds have been routinely used in industrial activities. The discharge of industrial effluents from various activities such as tanneries, electroplating, mining operations, dyeing, glass manufacture, battery manufacturing,

* Corresponding author.

chemical manufacturing, and pharmaceutical preparations is accountable for metallic pollutants in environmental aquatic bodies [2]. Primarily, Cr exists as Cr(III) and Cr(VI) ions [3]. Among these, Cr(III) is considered as an essential element for biological functioning in human [4], whereas Cr(VI) is toxic in nature, and regarded as a priority pollutant because of its non-biodegradability and accumulation features [5]. Cr(VI) is limited to 50 and 100 μg L^{-1} in drinking water by WHO and US-EPA, respectively. Therefore, treatment of Cr(VI) ions contaminated effluent prior to its discharge into environmental water bodies is mandatory for human health and environmental safety [6]. Various techniques such as adsorption [7–10], reduction [11–14], membrane separation [15–18], ion exchange [19–22], and electrochemical [23–25] have been in use for the treatment of Cr(VI) ions contaminated water. Among these techniques adsorption is considered as comparatively attractive because of operational simplicity, cost effective, high selectivity and sensitivity of the solid phases [26].

Layered double hydroxides (LDHs) are anionic clays, and generally represented as $[M_{1-x}^{2+}M_x^{3+}(OH)_2]^{x+}(A^{n-})_{x/n}\cdot mH_2O$. Where A^{n-} is an interlayer anion, M^{3+} is a trivalent cation, M^{2+} is a divalent cation. The charge on the layers depends on the M^{2+}/M^{3+} ratio, and x is the molar ratio of $M^{3+}/(M^{2+} + M^{3+})$. LDH is attractive adsorbent for adsorptive removal of pollutants/contaminations from wastewater samples because of its structural features, interlayered anions mobility, larger surface area, porosity, and high efficiency and selectivity [27]. In this study, CdCr-NO$_3$ LDH was synthesized, and applied as an efficient adsorbent for adsorptive removal/capturing of Cr(VI) ions from industrial effluents.

2. Materials and methods

2.1. Materials

Table 1 contains equipment and chemicals, used in this study. Double distilled water was used throughout the experiment. For statistical analysis, STATGRAPHICS software (version 16.1.11, 32 bit, Statpoint Technologies Incorporation, USA) was employed.

2.2. Synthesis of CdCr-NO$_3$ LDH

In a typical synthetic procedure, 250 mL of an aqueous solution, containing 0.05 mol L^{-1} Cd(NO$_3$)$_2$·4H$_2$O and 0.025 mol L^{-1} Cr(NO$_3$)$_3$ was prepared and poured into 1,000 mL of beaker. Another aqueous solution, 0.5 mol L^{-1} NaOH solution was added drop-wise into the solution of mixed metal salts with magnetically stirring at 50°C, maintaining pH at 9. A thick precipitated product was obtained which was filtered followed by repeated washing with de-ionized water until the pH of filtrate became neutral. The product CdCr-NO$_3$ LDH was oven-dried at 80°C for 8 h.

2.3. Factorial design

2.3.1. Variable factors and response

Independent variables which can affect the adsorption are called "factors". Whereas response is dependent variable which is adsorption (%) of Cr(VI) ions in this study.

For CCD model with n^k design, where is number of factors and n is number of levels. In this study, $k = 4$ (four factors: adsorbent dose, initial concentration, pH and shaking time) and $n = 2$ (two levels: minimum and maximum).

2.3.2. Experimental design

The n^k design with $k = 4$ and $n = 2$, formulated sixteen (16) adsorption experiments with two replicate as shown in Table 3. All the adsorption experiments were performed and results are summarized in Table 4.

2.4. Adsorption experiment

The adsorption experiment was carried out at optimum values of factors as predicted by CCD model. In a typical experiment, 50 mL bottle, contains 25 mL of 10 mg L^{-1} Cr(VI) ions of pH 4.0 and 40 mg of CdCr-NO$_3$ LDH adsorbent, was shaken at 120 rpm for 30 min at 25°C. The mixture was filtered, and filtrate was subjected to FAAS for Cr quantification. Adsorption of Cr(VI) ions was calculated by Eq. (1) and found to be 97.5% with RDS (%) ≤4.0.

$$\text{Adsorption}(\%) = \left(\frac{C_i - C_f}{C_i}\right) \times 100 \tag{1}$$

where C_i and C_f are the initial and final concentrations of Cr(VI) ions, respectively.

3. Results and discussion

3.1. Characterization

3.1.1. Fourier transform infrared spectroscopy

Stretching vibrations at 3,378.01 and 1,355.51 cm^{-1} in Fourier transform infrared (FT-IR) spectrum (Fig. 1) of CdCr-NO$_3$ LDH attributed to the hydroxyl moiety of LDH and water. Bending vibration at 1,641.47 cm^{-1} confirmed the presence of water. Stretching vibration at 1,355.51 cm^{-1} attributed to the nitrate anions. Stretching vibrations at 748.87 and 685.54 cm^{-1} attributed to M–O (Cd–O and Cr–O) linkage in LDH [28,29]. This spectral information revealed the formation CdCr LDH which was intercalated with nitrate anions and water molecules.

3.1.2. Powder X-ray diffraction

The characteristic diffraction peaks in the X-ray diffraction (XRD) pattern (Fig. 2) of CdCr-NO$_3$ LDH at 2θ values 15.10 and 26.02° correspond to (003) and (006) planes (hkl) of crystal system of the LDH, respectively, revealing the layered structure of CdCr-NO$_3$ LDH [30]. The basal (d) spacing of 003 and 006 planes were calculated and found to be 0.58 and 0.35 nm respectively. The broadness and noise is due to the least crystallinity of the synthesized material.

3.1.3. Energy-dispersive X-ray-scanning electron microscopy

Energy-dispersive X-ray analysis of CdCr-NO$_3$ LDH was carried out for elemental analysis. The material contained

Table 1
Equipment and chemicals used in the study

Items	Particulars	Brand/Company	Purposes
Equipment	Flame Atomic Absorption Spectrometer	PerkinElmer AAnalyst 800, USA	Quantification of metal ions
	Nicolet iS10 FT-IR Spectrometer	Thermo Fisher Scientific FT-IR Spectrometer, UK	FT-IR spectra recording
	D8 ADVANCE X-ray diffractometer, X-ray: Cu-Kα ($\lambda = 1.54056$ Å)	Bruker, Germany	XRD analysis
	Scanning electron microscope	JSM-6490LV, JEOL, Japan	SEM images scanning
	XFlash detector 4010 133 eV, X-ray: Cu-Kα ($\lambda = 1.5406$ Å)	Bruker, Germany	Energy-dispersive X-ray (EDX) analysis
	Shaker	Model No.1-4000, Germany	Shaking
	pH meter	inoLab pH 720, Germany	pH measurement
Chemicals (ACS reagent)	$Cd(NO_3)_2 \cdot 4H_2O$	Sigma-Aldrich, China	Synthesis
	$Cr(NO_3)_3$		
	NaOH		
	HCl/KCl, CH_3COOH/CH_3COONa	Sigma-Aldrich, China	Buffer solutions preparation
	NH_3/NH_4Cl		

Table 2
Factors and their levels for n^k design

Factors	Levels of factors		
	Minimum (−1)	Intermediate (0)	Maximum (+1)
A: Adsorbent dose (mg)	10	55.0	100
B: Concentration (mg L^{-1})	5	12.5	25
C: pH	2.0	05.5	9.0
D: Shaking time (min)	10	95.0	180

Table 3
Experimental design

Run No.	*A*	*B*	*C*	*D*
1	1	1	−1	1
2	0	1	0	0
3	1	1	1	−1
4	−1	1	−1	−1
5	−1	0	0	0
6	−1	−1	−1	−1
7	−1	1	1	1
8	0	0	−1	0
9	0	−1	0	0
10	1	−1	−1	1
11	1	−1	1	−1
12	0	0	0	1
13	−1	−1	1	1
14	0	0	0	−1
15	0	0	1	0
16	1	0	0	0
17	0	0	0	0
18	0	0	0	0

20.07, 72.75 and 7.18% of O, Cd(II) and Cr(III), respectively as shown in Fig. 3. Scanning electron microscopy (SEM) image (Fig. 4) of nanostructured CdCr-NO$_3$ LDH revealed that material is aggregated and porous. Clear layers of the synthesized material are seen in the image, which are highlighted.

3.1.4. Thermogravimetric analysis-differential scanning calorimetry

Thermal stability of CdCr-NO$_3$ LDH was investigated by thermogravimetric analysis (TGA) and differential scanning calorimetry (DSC). Thermogram (Fig. 5) revealed the fragmentation of CdCr-NO$_3$ LDH in three steps. First-step corresponds to surface-adsorbed-moisture loss at below 144.39°C, second-step corresponds to intercalated-water loss at 159.53–195.5°C (start-end) [31], and third Step corresponds to intercalated-nitrate loss and dehydroxylation of LDH sheets at 509.44–572.31°C (start-end) [32,33].

3.2. Effect of factors on adsorption

Fig. 6 depicts the individual effect factors. Adsorption (%) of Cr(VI) ions was slightly increased with increasing of adsorbent dosage, then became almost unchanged with further increasing of CdCr-NO$_3$ LDH amount, as the number of adsorbent-particles were increased for capturing of Cr(VI) ions. Adsorption (%) was declined with increasing of concentration, as the active sites onto the surface of adsorbent become occupied. The adsorption (%) was potentially

declined with increasing of pH as nitrated ions were de-intercalated in acidic medium, so the adsorbent became active for dichromate ions in acidic medium. The adsorption (%) was increased and then decreased with increasing of shaking time. The decreasing of adsorption was probably due to the possible desorption.

3.3. Analysis of variance

Analysis of variance (Table 5) suggests that all the effects, that is, main effects as well as interaction effects

except *BB*, *CD* and *DD* have $P < 0.05$, and high *F*-value, indicating the significant effect of these terms on response variable, that is, percentage adsorption at the 95.0% confidence level [34–36]. The R^2 statistic indicates that the CCD model was a good fit and explained 99.87% of the
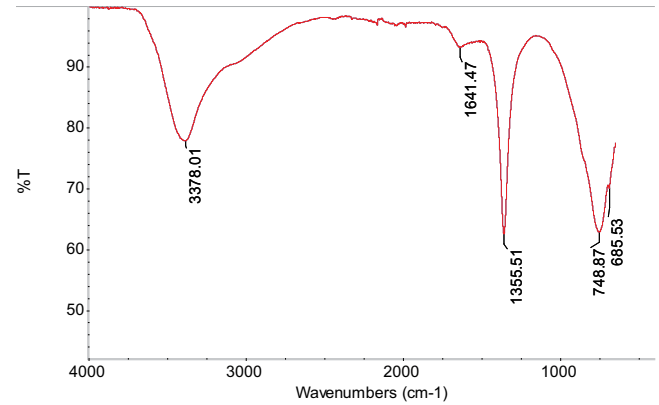
Table 4
Adsorption (%) of Cr(VI) ions at designed experiments

Run No.	Adsorption (%)			
	Observed	Fitted	Lower 95.0% CL	Upper 95.0% CL
1	93.0	93.1	91.6	94.5
2	88.3	88.3	86.9	89.7
3	88.9	88.9	87.5	90.3
4	92.5	92.7	92.1	93.3
5	99.7	99.8	99.4	98.9
6	93.2	92.7	92.1	93.3
7	86.0	86.4	85.3	87.5
8	89.7	89.6	88.2	91.0
9	97.3	97.3	95.9	98.7
10	95.5	95.5	94.1	96.9
11	98.5	98.5	97.2	99.9
12	84.4	84.3	82.9	85.7
13	97.1	96.8	95.7	97.8
14	99.3	99.4	98.0	99.8
15	88.8	88.8	87.4	90.2
16	96.3	96.4	95.0	97.8
17	90.8	90.7	89.3	92.1
18	83.6	83.5	82.1	84.9

CL: Confidence level

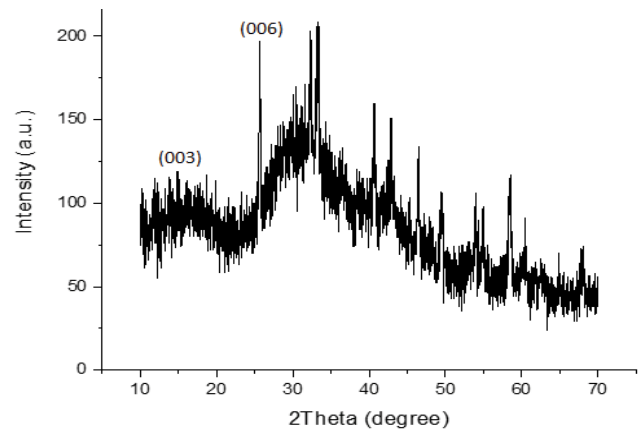Fig. 1. FT-IR spectrum of CdCr-NO$_3$ LDH.

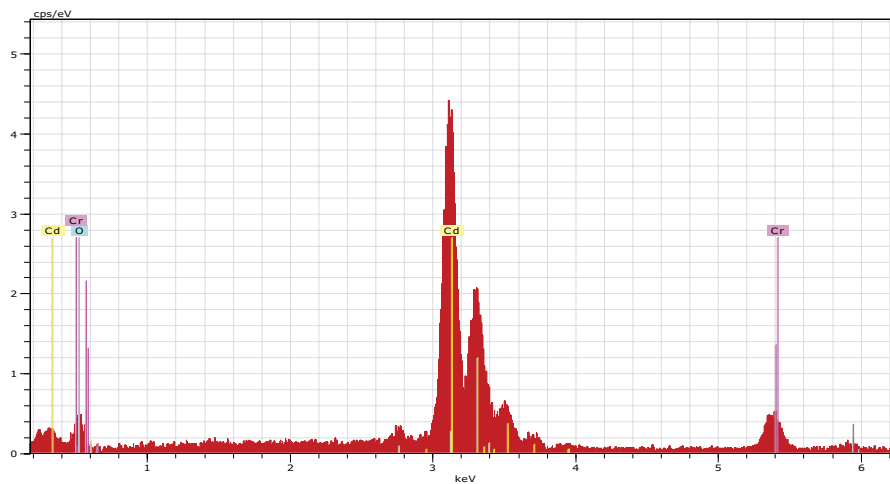Fig. 2. XRD pattern of CdCr-NO$_3$ LDH.

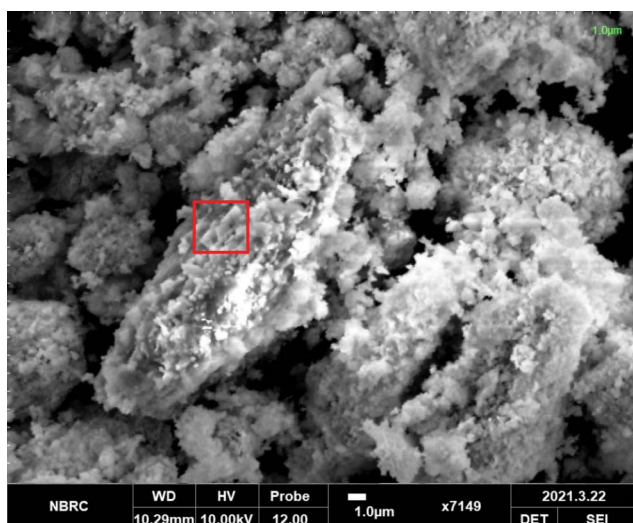Fig. 3. EDX spectrum of CdCr-NO$_3$ LDH.

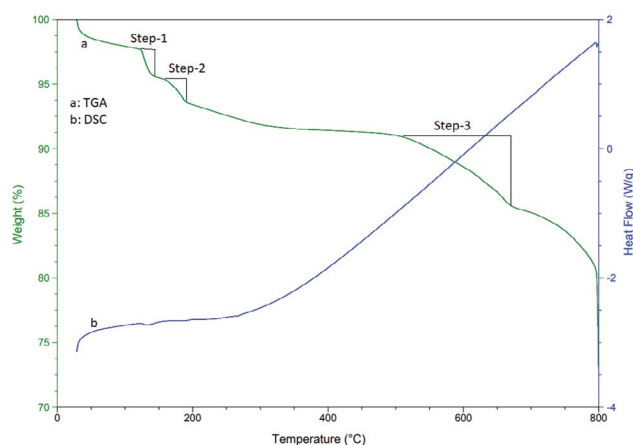Fig. 4. SEM image of CdCr-NO$_3$ LDH.

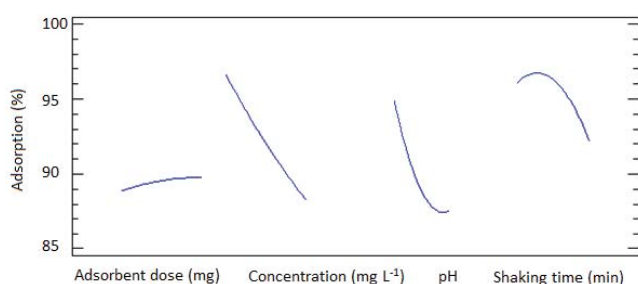Fig. 5. TGA-DSC curves of CdCr-NO$_3$ LDH.

Fig. 6. Effect of factors on the adsorption (%) of Cr(VI) ions.

variability in adsorptive removal (%). R^2 (adjusted) was 99.26%, which is more suitable for comparing model with different numbers of independent variables. The standard error of the estimate shows the standard deviation of the residuals, which was found to be 0.448193 and mean absolute error was found to be 0.132875.

Table 5
Analysis of variance

Factors	Sum of squares	DF	Mean squares	*F*-ratio	*P*-value
A	47.3701	1	47.3701	235.82	0.0006
B	35.1047	1	35.1047	174.76	0.0009
C	269.045	1	269.045	1,339.35	0.0000
D	26.0025	1	26.0025	129.45	0.0015
AA	2.39102	1	2.39102	11.90	0.0409
AB	20.8606	1	20.8606	103.85	0.0020
AC	3.07818	1	3.07818	15.32	0.0296
AD	31.3025	1	31.3025	155.83	0.0011
BB	0.44263	1	0.44263	1.44	0.2344
BC	67.9848	1	67.9848	338.44	0.0004
BD	29.7066	1	29.7066	147.88	0.0012
CC	3.18609	1	3.18609	15.86	0.0283
CD	1.82825	1	1.82825	1.10	0.5691
DD	1.49011	1	1.49011	2.42	0.7231
Total error	0.60263	3	0.20087	–	–
Total (corr.)	460.504	17	–	–	–

A: Adsorbent dosage (mg), *B*: Concentration (mg L^{-1}), *C*: pH, *D*: Shaking time (min), DF: Degree of freedom, R^2 = 99.87%, R^2 (adjusted for DF) = 99.26%, Standard error of estimate = 0.448193 and Mean absolute error = 0.132875.

Table 6
Factors and regression coefficients for the removal of Cr(VI) ions

Factors	Estimated coefficients
A: Amount	0.045399000
B: Concentration	−0.219141000
C: pH	3.444940000
D: Time	0.073107400
A^2	0.000480661
AB	0.001783110
AC	0.003938410
AD	−0.001156370
B^2	0.000206809
BC	−0.018508900
BD	0.001126510
C^2	−0.091720100
CD	−0.001606890
D^2	−0.000106351
Constant	60.23730000

3.4. Regression equation

Regression equation [Eq. (2)] with regression coefficients (Table 6) for removal/capturing of Cr(VI) ions is fitted well to the experimental data. By putting the coefficients in Eq. (2), the removal was calculated and found to be 98.6%.

$$\text{Removal}(\%) = 60.2373 + 0.0453998A - 0.219141B + 3.44494C + 0.0731074D + 0.000480661A^2 + 0.00178311AB$$
$$+ 0.00393841AC - 0.00115637AD + 0.000206809B^2 - 0.0185089BC + 0.00112651BD - 0.0917201C^2$$
$$- 0.00160689CD - 0.000106351D^2 \tag{2}$$

3.5. Effect of matrix ions

Performance of CdCr-NO$_3$ LDH adsorption of Cr(VI) ions was investigated in presence of Na$^+$, K$^+$, Mg^{2+}, Ca^{2+}, Cl$^-$, F$^-$, HCO$_3^-$, CO$_3^{2-}$, SO$_4^{2-}$, NO$_3^-$ and CH$_3$COO$^-$. The Cr(VI) ions were adsorbed (%) ≥95.5 ± ≤4.0 in presence of 500 mg L^{-1} individual cations, and 70.5–81.7 ± ≤3.5 in presence of 400 mg L^{-1} individual anions. The adsorption was decreased in presence of anions, which was probably due to the possible adsorption competition between anions and dichromate anions.

3.6. Equilibrium studies

Equilibrium experiments were performed by varying concentration (3.0–20 mg L^{-1}) of Cr(VI) ions, pH 3, adsorbent dosage 40 mg and shaking time 30 min at 25°C.

3.6.1. Langmuir isotherm

Mono-layer adsorption can be explained by use of Langmuir isotherm model, Eq. (3) shows the liner form of Langmuir model. An important Langmuir parameter is separation factor (R_L), which is represented by Eq. (4), respectively [34,37].

$$\frac{C_e}{C_{ads.}} = \frac{1}{Q}C_e + \frac{1}{Qb_L} \tag{3}$$

$$R_L = \frac{1}{1 + (b_L C_i)} \tag{4}$$

where C_e (mg L^{-1}) and C_{ads} (mg g^{-1}) are concentration of Cr(VI) ions at equilibrium and adsorbed amount respectively. Q (mg g^{-1}) is sorption capacity (monolayer) and b_L (L mg^{-1}) is Langmu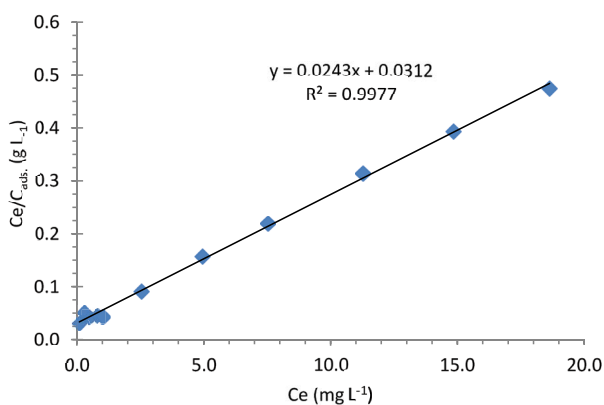ir constant. C_e/C_{ads} vs. C_e plot (Fig. 7) was found to be a good fit to the adsorption data with R^2 of 0.997. The Q of CdCr-NO$_3$ LDH for Cr(VI) ions was calculated and found to be 1,028.8 ± 2.5 mg g^{-1}. R_L values were calculated and found in the range of 0.37–0.89, revealing favorable adsorption of Cr(VI) ions onto CdCr-NO$_3$ LDH [34].

3.6.2. Freundlich isotherm

Eq. (5) represents the linear form of Freundlich isotherm, which was tested by plotting logC_{ads} vs. logC_e (Fig. 8). A good linear relationship with R^2 of 0.997 showed the good co-relation between both factors. Multi-layered sorption capacity (K_F) was calculated and found to be 595.6 ± 3.5 mg g^{-1}. While 1/n (dimensionless constant) is related to the adsorption intensity or energy, was calculated and found to be 0.172, revealing heterogeneously-distributed active sites onto the surface of adsorbent [34,37].

$$\log C_{ads} = \frac{1}{n}\log C_e + \log K_F \tag{5}$$

3.6.3. Dubinin–Radushkevich isotherm

Dubinin–Radushkevich isotherm (linear form), Polanyi potential (ε), and sorption energy (E) are is represented by Eqs. (6)–(8), respectively [38]. Dubinin–Radushkevich isotherm (Fig. 9) yielded R^2 of 0.998 showing good co-relation ε to the amount adsorbed. The total sorption capacity (K_{D-R}) was calculated from intercept (–0.7697) of the plot and was found to be 11.58 ± 3.0 mg g^{-1}. The E value calculated from the slope of the plot was 9.13 ± 2.5 kJ mol^{-1}, which is >8 kJ mol^{-1} showing the possibility of chemisorption or ion exchange sorption mechanism of Cr(VI) ions onto CdCr-NO$_3$ LDH [34].

$$\ln C_{ads} = \ln K_{D-R} - \beta\varepsilon^2 \tag{6}$$

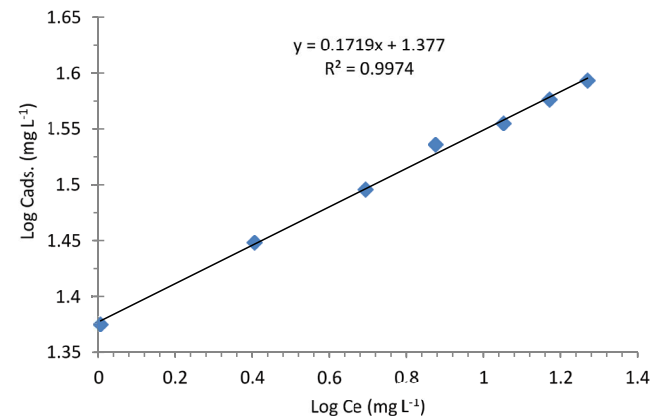Fig. 7. Langmuir isotherm for the adsorption of Cr(VI) ions onto CdCr-NO$_3$ LDH.

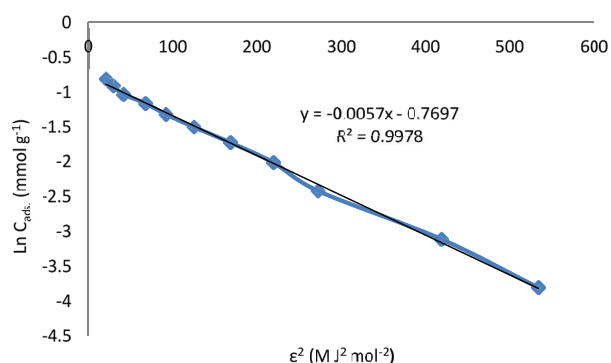Fig. 8. Freundlich isotherm for the adsorption of Cr(VI) ions onto CdCr-NO$_3$ LDH.

Fig. 9. Dubinin–Radushkevich isotherm for the adsorption of Cr(VI) ions onto CdCr-NO$_3$ LDH.

Table 7
Different LDHs adsorbents for Cr(VI) ions adsorption

Adsorbents	pH	Q (mg g^{-1})	K_F (mg g^{-1})	References
NiFe-NO$_3$ LDH	–	26.8	–	[40]
NiAl-NO$_3$ LDH	2.0	34.1	–	[41]
MgAl-NO$_3$ LDH	6.5	30.3	1.4	[42]
NiAl-NO$_3$ LDH	6.5	57.5	2.0	[42]
ZnAl-NO$_3$ LDH	6.5	68.1	1.7	[42]
MgAl-NO$_3$ LDH	6.0	71.9	18.4	[43]
CoAl-NO$_3$ LDH	2.0	109.5	8.6	[44]
MgAl-NO$_3$ LDH	8.1	14.3	1.5	[45]
CuFeCr-NO$_3$	2.0	22.2	22.2	[46]
CdCr-NO$_3$ LDH	4.0	1,028.8 ± 2.5	595.6 ± 3.5	This work

$$\varepsilon = RT \ln\left(1 + \frac{1}{C_e}\right) \tag{7}$$

$$E = \frac{1}{\sqrt{-2\beta}} \tag{8}$$

3.7. Different LDHs for Cr(VI) ions adsorption

Different LDHs adsorbents such as NiFe-NO$_3$, MgAl-NO$_3$, ZnAl-NO$_3$, CoAl-NO$_3$ and CuFeCr-NO$_3$, etc. have been applied for removal/capturing of Cr(VI) ions. As synthesized nanostructured CdCr-NO$_3$ LDH possessed comparatively high adsorption capacity for Cr(VI) ions from aqueous solutions as shown in Table 7.

3.8. Application of the method

CdCr-NO$_3$ LDH worked well for adsorptive removal of Cr(VI) ions form spiked wastewater samples. The Cr(VI) ions were removed ≥85.0% with RDS ≤2.4% (Table 8).

4. Conclusion

LDH is an attractive adsorbent for adsorptive removal of pollutants/contaminations from industrial effluents

Table 8
Removal of Cr(VI) ions from spiked wastewater samples

Sample	Added (mg L^{-1})	Found (mg L^{-1})	Removal (%) ± RSD (%)
S-I	0.0	ND	–
	5.0	4.9	98.0 ± 4.0
	10	9.7	97.0 ± 3.0
	20	18.0	90.0 ± 2.5
S-II	0.0	2.5	–
	5.0	7.3	96.0 ± 4.0
	10	12.4	99.0 ± 2.4
	20	19.5	85.0 ± 4.0

S-I: Tap water sample, collected from Research Laboratory, Institute of Chemistry University of Sindh Jamshoro 76080, Pakistan. S-II: Industrial effluent collection from Industrial Area in Hyderabad, Pakistan.

because of its structural features, interlayered anions mobility, larger surface area, porosity, and high efficiency and selectivity. XRD and analysis confirmed layered structured of the syntheses material, while IR spectroscopy confirmed the presence of intercalated nitrate anions in between sheets of LDH, which are exchangeable. Therefore Cr(VI) ions were adsorbed onto CdCr-NO$_3$ LDH by exchangeable mechanism as Cr(VI) exists as $Cr_2O_7^{2-}$ and $HCrO_4^-$ ions at pH ≤ 6.0 [39]. CCD model predicted the optimum values of factors for quantitative adsorption of the Cr(VI) ions.

References

[1] L. Zhou, G. Zhang, J. Tian, D. Wang, D. Cai, Z. Wu, Functionalized Fe$_3$O$_4$@C nanospheres with adjustable structure for efficient hexavalent chromium removal, ACS Sustainable Chem. Eng., 5 (2017) 11042–11050.

[2] Y.C. Sharma, V. Srivastava, Comparative studies of removal of Cr(VI) and Ni(II) from aqueous solutions by magnetic nanoparticles, J. Chem. Eng. Data, 56 (2011) 819–825.

[3] S. Zhou, B. Zhang, Z. Liao, L. Zhou, Y. Yuan, Autochthonous N-doped carbon nanotube/activated carbon composites derived from industrial paper sludge for chromate(VI) reduction in microbial fuel cells, Sci. Total Environ., 712 (2020) 136513, doi: 10.1016/j.scitotenv.2020.136513.

[4] R. Pechancová, J. Gallo, D. Milde, T. Pluháček, Ion-exchange HPLC-ICP-MS: a new window to chromium speciation in biological tissues, Talanta, 218 (2020) 121150, doi: 10.1016/j.talanta.2020.121150.

[5] Z. Lv, X. Tan, C. Wang, A. Alsaedi, T. Hayat, C. Chen, Metal-organic frameworks-derived 3D yolk shell-like structure Ni@carbon as a recyclable catalyst for Cr(VI) reduction, Chem. Eng. J., 389 (2020) 123428, doi: 10.1016/j.cej.2019.123428.

[6] C. Xiao, J. Lin, Efficient removal of Cr(VI) ions by a novel magnetic 4-vinyl pyridine grafted Ni$_3$Si$_2$O$_5$(OH)$_4$ multiwalled nanotube, ACS Omega, 5 (2020) 23099–23110.

[7] G. Chen, C. Qiao, Y. Wang, J. Yao, Synthesis of magnetic gelatin and its adsorption property for Cr(VI), Ind. Eng. Chem. Res., 53 (2014) 15576–15581.

[8]   J. Tan, Y. Song, X. Huang, L. Zhou, Facile functionalization of natural peach gum polysaccharide with multiple amine groups for highly efficient removal of toxic hexavalent chromium (Cr(VI)) ions from water, ACS Omega, 3 (2018) 17309–17318.

[9]   M.A. Salam, M.R. Abukhadra, A. Adlii, Insight into the adsorption and photocatalytic behaviors of an organo-bentonite/Co₃O₄ green nanocomposite for malachite green synthetic dye and Cr(VI) metal ions: application and mechanisms, ACS Omega, 5 (2020) 2766–2778.

[10] T.D. Ntuli, T.H. Mongwe, L.L. Sikeyi, O. Mkhari, N.J. Coville, E.N. Nxumalo, M.S. Maubane-Nkadimeng, Removal of hexavalent chromium via an adsorption coupled reduction mechanism using olive oil derived carbon nano-onions, Environ. Nanotechnol. Monit. Manage., 16 (2021) 100477, doi: 10.1016/j.enmm.2021.100477.

[11] A. Olad, R. Nabavi, Application of polyaniline for the reduction of toxic Cr(VI) in water, J. Hazard. Mater., 147 (2007) 845–851.

[12] M. Gan, D. Huang, F. Chen, K. Zhang, J. Zhu, Enhanced Cr(VI) reduction and Cr(III) co-precipitation through the synergistic effect between sulfide minerals and chemoautotrophic decomposer, J. Environ. Chem. Eng., 9 (2021) 105942, doi: 10.1016/j.jece.2021.105942.

[13] B. Li, P. Liao, L. Xie, Q. Li, C. Pan, Z. Ning, C. Liu, Reduced NOM triggered rapid Cr(VI) reduction and formation of NOM-Cr(III) colloids in anoxic environments, Water Res., 181 (2020) 115923, doi: 10.1016/j.watres.2020.115923.

[14] M. Wei, G. Jian, C. Zhen, H. Jinglu, X. Gang, P. Yuzhen, Z. Zhe, T. Dazhi, A new method of Cr(VI) reduction using SiC doped carbon electrode and Cr(III) recovery by hydrothermal precipitation, Colloids Surf., A, 610 (2021) 125724, doi: 10.1016/j.colsurfa.2020.125724.

[15] H. Peng, J. Guo, Removal of chromium from wastewater by membrane filtration, chemical precipitation, ion exchange, adsorption electrocoagulation, electrochemical reduction, electrodialysis, electrodeionization, photocatalysis and nanotechnology: a review, Environ. Chem. Lett., 18 (2020) 2055–2068.

[16] R. Goswami, A. Mishra, N. Bhatt, A. Mishra, P. Naithani, Potential of chitosan/nanocellulose based composite membrane for the removal of heavy metal (chromium ion), Mater. Today: Proc., 46 (2021) 10954–10959.

[17] O. Njoya, S. Zhao, X. Kong, J. Shen, J. Kang, B. Wang, Z. Chen, Efficiency and potential mechanism of complete Cr(VI) removal in the presence of oxalate by catalytic reduction coupled with membrane filtration, Sep. Purif. Technol., 275 (2021) 118915, doi: 10.1016/j.seppur.2021.118915.

[18] S. Roy, S. Majumdar, G.C. Sahoo, S. Bhowmick, A.K. Kundu, P. Mondal, Removal of As(V), Cr(VI) and Cu(II) using novel amine functionalized composite nanofiltration membranes fabricated on ceramic tubular substrate, J. Hazard. Mater., 399 (2020) 122841, doi: 10.1016/j.jhazmat.2020.122841.

[19] H. Wang, X. Song, H. Zhang, P. Tan, F. Kong, Removal of hexavalent chromium in dual-chamber microbial fuel cells separated by different ion exchange membranes, J. Hazard. Mater., 384 (2020) 121459, doi: 10.1016/j.jhazmat.2019.121459.

[20] E. Jashni, S.M. Hosseini, Promoting the electrochemical and separation properties of heterogeneous cation exchange membrane by embedding 8-hydroxyquinoline ligand: chromium ions removal, Sep. Purif. Technol., 234 (2020) 116118, doi: 10.1016/j.seppur.2019.116118.

[21] X. Yaqiang, L. Ju, L. Jun, L. Minghong, F. Yawen, W. Hongtao, T. Song, L. Jun, Hypercrosslinked mesoporous poly(ionic liquid)s with high density of ion pairs: efficient adsorbents for Cr(VI) removal via ion-exchange, Chem. Eng. J., 378 (2019) 122107, doi: 10.1016/j.cej.2019.122107.

[22] S.W. Ahmad, M.S. Zafar, S. Ahmad, M. Zia-Ul-Haq, M. Ashraf, J. Rabbani, S. Ullah, Removal of chromium(VI) from wastewater through ion exchange, kinetic and scale up studies, Environ. Prot. Eng., 45 (2019) 17–29.

[23] B. Butter, P. Santander, G.D. Pizarro, D.P. Oyarzún, F. Tasca, J. Sánchez, Electrochemical reduction of Cr(VI) in the presence of sodium alginate and its application in water purification, J. Environ. Sci., 101 (2021) 304–312.

[24] X. Yang, L. Liu, M. Zhang, W. Tan, G. Qiu, L. Zheng, Improved removal capacity of magnetite for Cr(VI) by electrochemical reduction, J. Hazard. Mater., 374 (2019) 26–34.

[25] F. Yao, M. Jia, Q. Yang, K. Luo, F. Chen, Y. Zhong, L. He, Z. Pi, K. Hou, D. Wang, X. Li, Electrochemical Cr(VI) removal from aqueous media using titanium as anode: Simultaneous indirect electrochemical reduction of Cr(VI) and in-situ precipitation of Cr(III), Chemosphere, 260 (2020) 127537, doi: 10.1016/j.chemosphere.2020.127537.

[26] K. Zhu, C. Chen, S. Lu, X. Zhang, A. Alsaedi, T. Hayat, MOFs-induced encapsulation of ultrafine Ni nanoparticles into 3D N-doped graphene-CNT frameworks as a recyclable catalyst for Cr(VI) reduction with formic acid, Carbon, 148 (2019) 52–63.

[27] F. Qianzhen, S. Ye, H. Yang, K. Yang, J. Zhou, Y. Gao, Q. Lin, X. Tan, Z. Yang, Application of layered double hydroxide-biochar composites in wastewater treatment: recent trends, modification strategies, and outlook, J. Hazard. Mater., 420 (2021) 126569, doi: 10.1016/j.jhazmat.2021.126569.

[28] D.A. Islam, K. Barman, S. Jasimuddin, H. Acharya, Synthesis of ultrasmall and monodisperse sulfur nanoparticles intercalated CoAl layered double hydroxide and their electrocatalytic water oxidation reaction at neutral pH, Nanoscale, 11 (2019) 7560–7566.

[29] W. Li, A. Liu, H. Tian, D. Wang, Controlled release of nitrate and molybdate intercalated in Zn-Al-layered double hydroxide nanocontainers towards marine anticorrosion applications, Colloid Interface Sci. Commun., 24 (2018) 18–24.

[30] B. Benalioua, M. Mansour, A. Bentouami, B. Boury, E.H. Elandaloussi, The layered double hydroxide route to Bi–Zn co-doped TiO₂ with high photocatalytic activity under visible light, J. Hazard. Mater., 288 (2015) 158–167.

[31] L.D.S. Neto, C.G. Anchieta, J.L.S. Duarte, L. Meili, J.T. Freire, Effect of drying on the fabrication of MgAl layered double hydroxides, ACS Omega, 6 (2021) 21819–21829.

[32] L.P.F. Benício, V.R.L. Constantino, F.G. Pinto, L. Vergütz, J. Tronto, L.M. da Costa, Controlled release of phosphate from layered double hydroxide structures: dynamics in soil and application as smart fertilizer, ACS Sustainable Chem. Eng., 6 (2017) 5152–5161.

[33] S. Rafique, A.K. Kasi, J.K. Kasi, Aminullah, M. Bokhari, Z. Shakoor, Fabrication of silver-doped zinc oxide nanorods piezoelectric nanogenerator on cotton fabric to utilize and optimize the charging system, Nanomater. Nanotechnol., 10 (2020) 1–12.

[34] B.A. Baig, A. Elçi, A.N. Siyal, S. Dehrajd, Q.K. Panhwar, A. Ahmed, A.R. Bhattia, F. Ali, M.Y. Khuhawar, Facile synthesis and characterization of β-Cd(OH)₂ nanostructures for adsorptive removal of Cr(VI) ions from wastewater: a statistical approach for multivariate sorption optimization, Desal. Water Treat., 218 (2021) 270–280.

[35] I.A. Bhatti, N. Ahmad, N. Iqbal, M. Zahid, M. Iqbal, Chromium adsorption using waste tire and conditions optimization by response surface methodology, J. Environ. Chem. Eng., 5 (2017) 2740–2751.

[36] S.H. Hasan, P. Srivastav, M. Talat, Biosorption of Pb(II) from water using biomass of *Aeromonas hydrophila*: central composite design for optimization of process variables, J. Hazard. Mater., 168 (2009) 1155–1162.

[37] D. Kundu, S.K. Mondal, T. Banerjee, Development of β-cyclodextrin-cellulose/hemicellulose-based hydrogels for the removal of Cd(II) and Ni(II): synthesis, kinetics, and adsorption aspects, J. Chem. Eng. Data, 64 (2019) 2601–2617.

[38] S.Q. Memon, S.M. Hasany, M.I. Bhanger, M.Y. Khuhawar, Enrichment of Pb(II) ions using phthalic acid functionalized XAD-16 resin as a sorbent, J. Colloid Interface Sci., 291 (2005) 84–91.

[39] O. Dvoynenko, S.L. Lo, Y.J. Chen, G.W. Chen, H.M. Tsai, Y.L. Wang, J.K. Wang, Speciation analysis of Cr(VI) and Cr(III) in water with surface-enhanced Raman Spectroscopy, ACS Omega, 6 (2021) 2052–2059

[40] Y. Lu, B. Jiang, L. Fang, F.L. Ling, J.M. Gao, F. Wu, X.H. Zhang, High performance NiFe layered double hydroxide for methyl orange dye and Cr(VI) adsorption, Chemosphere, 152 (2016) 415–422.

[41] S.X. Chen, Y.F. Huang, X.X. Han, Z.L. Wu, C. Lai, J. Wang, Q. Deng, Z.L. Zeng, S.G. Deng, Simultaneous and efficient removal of Cr(VI) and methyl orange on LDHs decorated porous carbons, Chem. Eng. J., 352 (2018) 306–315.

[42] W.W. Wang, J.B. Zhou, G. Achari, J.G. Yu, W.Q. Cai, Cr(VI) removal from aqueous solutions by hydrothermal synthetic layered double hydroxides: adsorption performance, coexisting anions and regeneration studies, Colloids Surf., A, 457 (2014) 33–40.

[43] M. Khitous, Z. Salem, D. Halliche, Effect of interlayer anions on chromium removal using Mg–Al layered double hydroxides: kinetic, equilibrium and thermodynamic studies, Chin. J. Chem. Eng., 24 (2016) 433–445.

[44] N. Jarrah, N.D. Mu'azu, M. Zubair, M. Al-Harthi, Enhanced adsorptive performance of Cr(VI) onto layered double hydroxide-bentonite composite: isotherm, kinetic and thermodynamic studies, Sep. Sci. Technol., 55 (2020) 897–1909.

[45] S. Zhao, Z. Li, H. Wang, H. Huang, C. Xia, D. Liang, J. Yang, Q. Zhang, Z. Meng, Effective removal and expedient recovery of As(V) and Cr(VI) from soil by layered double hydroxides coated waste textile, Sep. Purif. Technol., 263 (2021) 118419, doi: 10.1016/j.seppur.2021.118419.

[46] Y. Zhang, C. Jing, J. Zheng, H. Yu, Q. Chen, L. Guo, D. Pan, N. Naik, Q. Shao, Z. Guo, Microwave hydrothermal fabrication of CuFeCr ternary layered double hydroxides with excellent Cr(VI) adsorption, Colloids Surf., A, 628 (2021) 127279, doi: 10.1016/j.colsurfa.2021.127279.